CHAPTER 6

Performance of Resonant Sensors

by: Albert Prak, MESA Research Institute, University of Twente, Enschede, the Netherlands

6.1 Introduction

The behaviour of resonant sensors described in chapters 3 and 5 is rather ideal. In practice, there are a large number of physical effects which have an unwanted or uncontrollable effect on the mechanical transfer function of the system. Some of the effects meant in this framework are:

- Quality factors (damping)
- Shifts of the resonance frequency by mass loading
- Non-linear (large amplitude) effects
- Heating of the resonator
- Temperature effects

In the following sections, we will discuss some of these effects.

6.2 Quality factors [1]

The mechanical quality factor Q is a measure for the energy losses of the resonator or in other words, a measure for the mechanical damping. The Q-factor is defined as

$$Q \equiv 2\pi \frac{\text{maximum energy stored in one period}}{\text{dissipated energy per period}} \qquad (.15)$$

Low energy losses imply a high Q-factor. The Q-factor cannot be determined directly, but instead can be deduced from the response characteristics of the resonator. One common method of determining Q is from the steady state frequency response plot of a resonator excited by a harmonic force with constant amplitude(see fig 1)

$$Q \approx \frac{\omega_{res}}{\Delta\omega_{3\,dB}} \qquad (16)$$

where ω_{res} is the resonant frequency, defined as the frequency of maximum amplidude response, and $\Delta\omega_{3\,dB}$ is the half power bandwidth of the frequency response. Eq. (.16) indicates that Q is a measure for the sharpness or the frequency selectivity of the resonator. A high Q-factor means a sharp resonance peak. A high Q-factor for a resonant force gauge has several advantages: The energy required to maintain oscillation is kept low, which reduces heat generation and opens up the possibility of powering the resonant gauges from alternative sources. e.g., solar energy. Further, a high Q means a good frequency stability and the effects of the electronic circuitry, used to sustain the oscillation, on the oscillation frequency are minimized.

Several mechanisms of energy loss can be identified: (a) losses into the surrounding (fluid) medium, caused by acoustic radiation and viscous drag, (b)

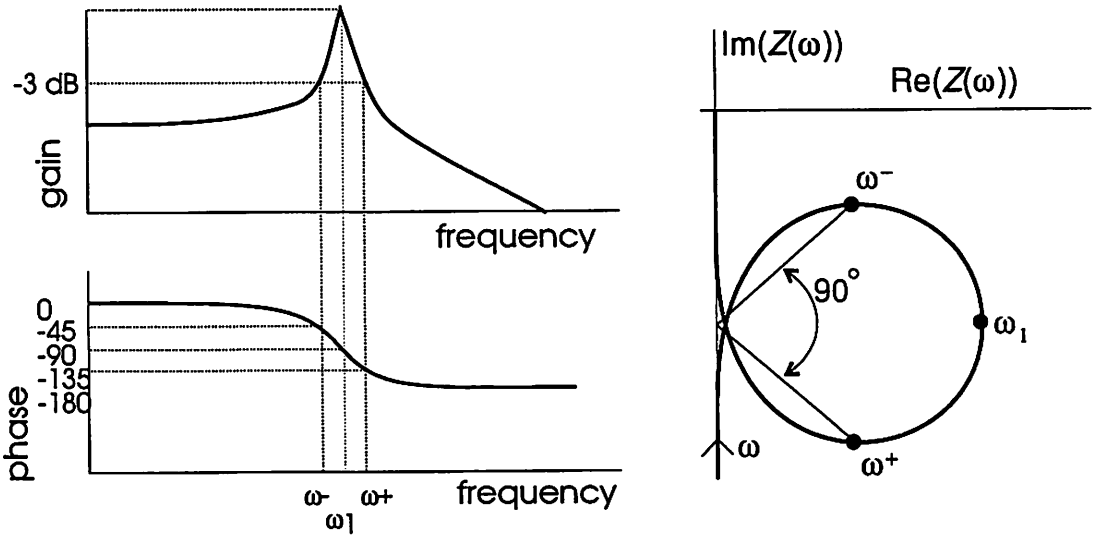

fig 1: determination of the quality factor from the bode-diagram (left) and from the polar plot

[1]From: H.A.C. Tilmans, *Micromechanical sensors using encapsulated built-in resonant strain gauges*, PhD Thesis chapter 2.4, Univ. of Twente, Enschede, the Netherlands (1993)

Also published in: H.A.C. Tilmans, M. Elwenspoek and J.H.J. Fluitman, *Micro resonant force gauges*, Sensors and Actuators A 30 (1992), 35-53.

lossed into the mount, used to support the resonator, due to motion of the mount, and (c) intrinsic damping caused by energy losses inside the material of the resonator. The energy loss of each loss mechanism separately can be described by a corresponding quality factor Q_i and the overal quality factor Q_{tot} can be found from

$$\frac{1}{Q_{tot}}=\sum_i \frac{1}{Q_i} \qquad (17)$$

It is obvious from the above equation, that Q_{tot} cannot exceed the value of the smallest Q_i. The discussion below mainly deals with vibrating beams. Quality factors of vibrating diaphragms are discussed elsewhere [31].

The losses into the surrounding fluid are due to viscous damping and/or radiation of sound waves propagating in a direction normal to the surface. The latter effect will only be significant if the acoustic wavelength becomes equal to or less than a typical dimension of the resonator [32, 33]. Acoustic radiation can generally be ignored for micromechanical resonators. Viscous damping is characterized by two contributions [34- 36]. One is due to the usual Stokes drag force for a body in uniform motion through a viscous fluid. The second (dynamic) part, the so-called *shear wave effect*, is characterized by a boundary layer around the vibrating structure and is dependent on the frequency of vibration ω, and further on the density ρ_0 and viscosity η of the fluid medium. The quality factor $Q_{viscous}$ caused by viscous damping can be expressed as [37]

$$Q_{viscous}=\frac{\rho A \omega}{c\left(\frac{R}{\delta(\eta,\rho_0,\omega)},\eta\right)} \qquad (18)$$

where c the coefficient of the dissipative part of the drag force, R represents the relevant linear dimension and $\delta=\sqrt{(2\eta/\rho_0\omega)}$ the characteristic width of the boundary layer. If δ is much larger than the linear dimensions of the resonator, the shear wave effects can be ignored and c is a given constant, dependent only on η: $Q_{viscous}=\rho A\omega/c(\eta)$, stating that in this case the quality factor is linearly proportional to the frequency of vibration. The viscous quality factor of a wide beam with a rectangular cross section and for zero applied axial force can then be expressed as

$$Q_{viscous,\,n}=\frac{\rho A \omega_n}{c(\eta)}=\frac{\alpha_n^2 b}{c(\eta)\sqrt{12}}\left(\frac{h}{l}\right)^2\sqrt{\frac{\rho E}{(1-\nu^2)}} \qquad (\delta \gg R) \qquad (19)$$

Form the above expression, it is seen that the viscous quality factor is inversely proportional to the aspect ratio (l/h) of the beam. Assuming $c(\eta)\approx 24\eta$, for a prismatic beam with a rectangular cross section [38], a viscous quality factor in

air (η=1.8x10^{-5} Ns/m^2) for the fundamental mode, of approximately 30 is found, for a silicon beam of 1 μm wide and an aspect ratio of 100. If shear wave effects cannot be ignored the quality factor will be lower and will become directly proportional to $\sqrt{\omega}$. This dependence has been experimentally observed by Lammerink *et al.* [.39] and Blom *et al.* [37].

In the discussion above, it was assumed that the resonator is isolated in space. If the flexurally vibrating resonator is close to an another stationary surface, damping forces increase due to a pressure built-up in the intervening space, i.e., the (air)gap [.38, .40, 41]. This so-called *squeeze-film damping* effect becomes significant if the gap spacing approaches or becomes less than the width of the vibrating beam. Whereas the viscous quality factor would be on the order of 100-2000 for an isolated beam, it rapidly drops below 1 if the gap spacing is too small. This has been experimentally observed by Howe *et al.* [41]. Squeeze-film damping can be slightly reduced by making ventilation holes in the vibrating beam [41, 42] or practically eliminated by placing the beam in an evacuated cavity [24, .27, .43].

The energy coupled into the supporting structure can be minimized by mechanically isolating the resonator from the mount . An example of a geometry providing a means of decoupling of a flexurally vibrating *single beam* from the support is an isolation system in between the beam and the support, consisting of a large mass and an isolator beam, acting as a soft spring-mass system with a natural frequency which is much lower than the frequency of the beam and of the support [.44, .45]. In this design, moment and shear reactions are isolated from the support, resulting in a reduction of energy losses. The mass has to be large to give it enough rotary inertia to form an efficient clamping edge for the resonating beam. A decoupling method for a torsional resonator was reported on by Buser *et al.* [46]. In their structure, a frame was designed around the resonator which itself can vibrate in a torsional mode. Again, the aim of the design was to have a high ratio of the resonant frequencies of the resonator and the mounting frame in order to minimize the energy losses. Quality factors in vacuum as high as 600,000 were measured for a structure made out of single crystalline silicon. Another way of lowering the energy losses into the support is by using a specific resonator design. A well known example is the *double ended tuning fork (DETF)*, consisting of two beams vibrating 180° out of phase thereby cancelling moment reactions at the beam roots and thus resulting in a reduction of energy losses, see Fig. 2. (a) [47]. The *triple beam* structure provides yet another way of cancelling moments and shear forces at the clamped ends, see Fig. 2 (b) [48, 49]. It consists of three beams. The middle beam is twice the width of the outer beams. The middle beam and the two outer beams vibrate 180 ° out of phase, resulting in the desired cancellation of moments and shear forces. This structure is very attractive from a fabricational point of view. It can easily be fabricated with the planar micromachining technologies and the excita-

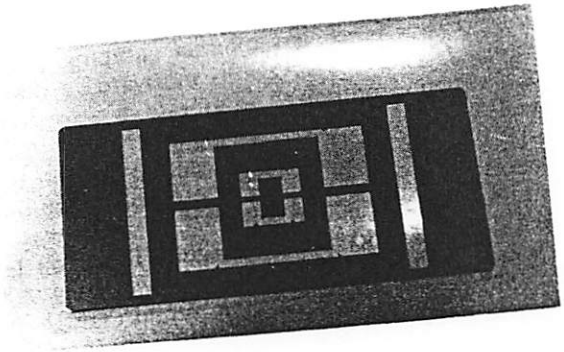

[46]

tion/detection of the flexural transverse (perpendicular to the substrate) vibrations does not mean any more difficulties as for the single beam approach.

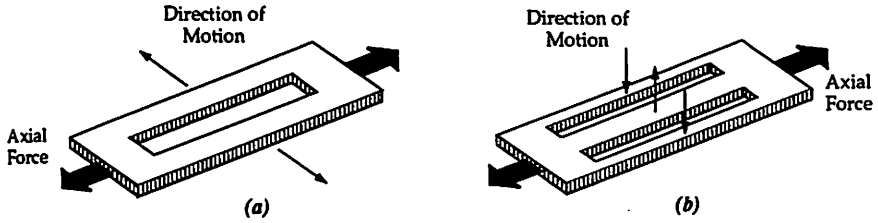

Fig. 2 (a) Double-ended tuning fork [2.47]; (b) Triple beam structure [2.48].

This in contrast to the DETF which requires in-plane excitation/detection schemes. Another structure, consisting of a balanced dual-diaphragm was reported on by Stemme *et al.* [42]. Here, a balanced torsional mode of vibration is excited, where energy losses into the mount are small due to a stationary center of mass and because the vibrating element is suspended at the nodal lines, which minimizes the movement of the mount. Balanced structures were reviewed by Stemme

Besides the external sources of energy losses described above, there still remains a large number of mechanisms through which vibrational energy can be dissipated within the material which is cyclically deformed. They include effects such as magnetic effects (magnetoelastic hysteresis), thermal effects (thermoelastic internal friction [50]), atomic reconstructions (dislocations, stress relaxation at grain boundaries) [.51]. A way of describing viscoelastic material losses or structural damping is by introducing a complex Young's modulus $E^*=E(1+i\gamma)$, where $i=\sqrt{-1}$ and γ is the structural damping factor [.52, .53]. The quality factor Q_{int} associated with structural damping is simply given by: $Q_{int}=1/\gamma$. Single crystal materials, such as quartz and single crystalline silicon, seem to have lower intrinsic losses compared to amorphous or poly-crystalline materials, and are therefore more attractive as a resonator material [54]. A lot of work however remains in investigating the damping properties of materials.

In describing the air pressure dependence of the overal quality factor Q_{tot}, three main pressure regions can be distinguished [.37, 38]. The transition points of these regions depend on the shape and material properties of the resonator and also on the way the resonator is supported. In general, near atmospheric pressure, viscous damping is the dominating mechanism. This region can be divided into two subregions, depending on the relative width of the boundary layer δ as discussed before. At high pressures and for high frequencies, shear wave effects dominate and Q_{tot} will be proportional to δ and thus to $1/\sqrt{p}$, where the p the air pressure. At lower pressures and/or frequencies, Q_{tot} will be independent of δ and thus independent of p. Lowering the pressure even further the Knudsen gas region is reached and the air no longer acts as a viscous fluid. Energy losses are now caused by individual collisions of the gas molecules with the resonator. In this region, Q_{tot} is proportional to $1/p$ [37, .55]. At very low pressures (e.g., <1 Pa) air damping can be ignored and the quality factor is determined by the losses into support and by the intrinsic losses, making Q_{tot} independent of p. Thus, in order to obtain a Q-factor as high as possible, vacuum encapsulation of the resonator is necessary.

References to 6.2

31 A. Prak, F. R. Blom, M. Elwenspoek and T. S. J. Lammerink, Q-factor and frequency shift of resonating silicon diaphragms in air, *Sensors and Actuators A, 25-27* (1991) 691-698.

32 W. K. Blake, The radiation from free-free beams in air and in water, *J. of Sound and Vibration,* 33 (1974) 427-450.

33 R. K. Jeyapalan and E. J. Richards, Radiation efficiencies of beams in flexural vibration, *J. of Sound and Vibration, 67*(1979) 55-67.

34 M. Christen, Air and gas damping of quartz tuning forks, *Sensors and Actuators,* 4 (1983) 555-564.

35 T. Terasawa, Y. Kawamura, K. Sato and S. Tanaka, Pressure dependent dynamic characteristics of miniature silicon oscillator, *Bull. Japan Soc. of Prec. Engg., 22* (1988) 49-54.

36 L. D. Landau and E. M. Lifshitz, *Fluid mechanics,* Pergamon Press, 2nd ed. (1963), ch. 2.

37 F. R. Blom, S. Bouwstra, M. Elwenspoek and J. H. J. Fluitman, Dependence of the quality factor of micromachined silicon beam resonators on pressure and geometry, *J. Vac. Sci. Techn. B, 10* (1992) 19-26.

38 W. E. Newell, Miniaturization of tuning forks, *Science, vol. 161* (1968) 1320-1326.

39 T. S. J. Lammerink, M. Elwenspoek and J. H. J. Fluitman, Thermal actuation of clamped silicon microbeams, *Sensors and Materials, 3,* 2 (1991), to be publised.

40 J. B. Starr, Squeeze-film damping in solid-state accelerometers, *Proc. IEEE Solid-State Sensors and Actuators Workshop, Hilton Head Island, SC, U.S.A., June 4-7, 1990,* pp. 44-47.

41 R. T. Howe and R. S. Muller, Resonant-microbridge vapor sensor, *IEEE Trans. Electron Devices, ED-33* (1986) 499-506.

42 E. Stemme and G. Stemme, A balanced resonant pressure sensor, *Sensors and Actuators, A21-A23* (1990) 336-341.

43 H. Guckel, J. J. Sniegowski, T. R. Christenson and F. Raissi, The application of fine-grained, tensile polysilicon to mechanically resonant transducers, *Sensors and Actuators, A21 - A23* (1990) 346-351.

44 W. C. Albert, Force sensing using quartz crystal flexure resonators, *Proc. 38th Annual Frequency Control Symposium - 1984,* pp. 233-239.

45 W. C. Albert, A low cost force sensing crystal resonator applied to weighing, *Proc. 42nd Annual Frequency Control Symposium - 1988, Baltimore, June 1-3, 1988,* pp. 78-84.

46 R. A. Buser and N. F. Rooij, Very high Q-factor resonators in monocrystalline silicon, *Sensors and Actuators, A21-A23* (1990) 323-327.

47 T. Ueda, F. Kohsaka and E. Ogita, Precision force transducers using mechanical resonators, *Measurement, 3,* (1985) 89-94.

48 R. G. Kirman, A vibrating quartz force sensor, *Transducers Tempcon Conference Papers 1983, London, 14-16 June, 1983,* 24 pp.

49 D. W. Satchell and J. C. Greenwood, A thermally-excited silicon accelerometer, *Sensors and Actuators, 17* (1989) 241-245.

50 T. V. Roszhart, The effect of thermoelastic internal friction on the Q of micromachined silicon resonators, *Proc. IEEE Solid-State Sensor and Actuator Workshop, Hilton Head Island, SC, USA, June 4-7, 1990,* pp. 13-16.

51 A. Muszynska, Internal damping in mechanical systems, *Dynamika Maszyn,* Polish Acad. Sci., Ossolineum, Warsaw (1974) 164-212 (in polish).

52 W. T. Thomson, *Theory of vibration with applications,* Prentice-Hall Inc., Englewood Cliffs, N. J., U. S. A., 2nd edition (1981) pp. 74-75.

53 R. E. D. Bishop, The treatment of damping forces in vibration theory, *J. of the Royal Aeronautical Society, 59* (1955) 738-742.

54 B. Hök and K. Gustafsson, Vibration analysis of micromechanical elements, *Sensors and Actuators, 8* (1985) 235-243.

55 R. G. Christian, The theory of oscillating-vane vacuum gauges, *Vacuum, 16* (1966) 175-178.

6.3 Loaded and unloaded quality factors [2]

6.3.1 Introduction

Determination of the quality factor based on pure mechanical considerations can be incorrect if the resonator is driven, or its vibration is sensed by mechanisms of the reversible type. For determination of the quality factor, energy dissipated at *any* port should be considered. When reversible mechanisms are used, energy can also be dissipated at the electrical ports by a resistive load. In this context, the term 'loaded Q' is in vogue. Two parameters are extremely important for the loaded Q, namely the electromechanical coupling factor k and the load at the electric ports Z_{load}. In fig. 6.3.1, the loaded Q is plotted in terms of the coupling factor k as a function of the complex load impedance Z_{load}. The minimum Q ($Q=2/k^2$) is obtained for $\mathrm{Im}(Z_{load}) = 0$. For non zero values of $\mathrm{Im}(Z_{load})$, which can be caused by parasitic capacitances, the minimum achievable value of the loaded Q decreases, and the value of Re (Z_{load}) corresponding to this minimum value changes.

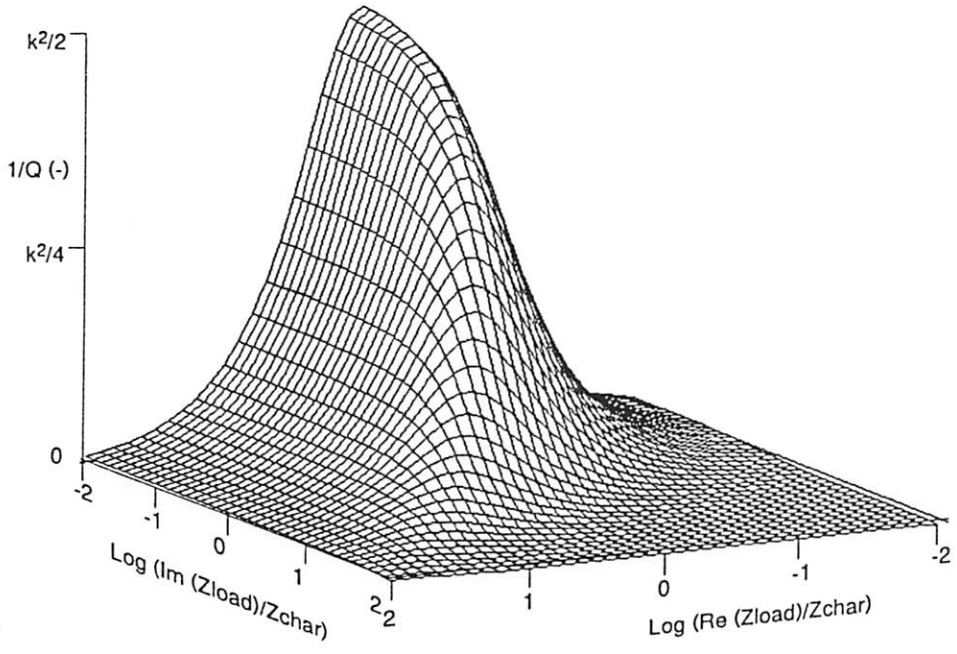

Fig. 6.3.1: $1/Q_{loaded}$ as a function of the complex load impedance Z_{load}.

6.3.2 The piezoelectric resonator

Let us consider the piezoelectrically operated force sensor [1,2]. The electromechanical coupling factor of this device is approximately $k \approx 0.01$, while the characteristic impedance $|1/j\omega C_{ZnO}| \approx 330$ kΩ at the first resonance frequency, which is 11 kHz. Maximum electrical power (minimum Q) will be dissipated when the load is 330 kΩ (resistive). In that case, the loaded Q will be $Q = 2/k^2 = 2 \cdot 10^4$. Since there are two electrical ports, which both can be loaded characteristically the minimum loaded Q that can be obtained with this device equals Q

---

[2] From: A. Prak, *Silicon resonant sensors: Operation and Response*, PhD Thesis, Univ. of Twente, Enschede, the Netherlands.

= 10^4. Since the mechanical Q (due to air damping and structural damping) is much lower (typical value in air is $100 < Q < 1000$) the electrical load will not have much effect on the Q of the force sensor. In fig. 6.3.2, we plotted the system Q (electrical and mechanical damping) as a function of the electric load (resistive) for various values of the mechanical Q.

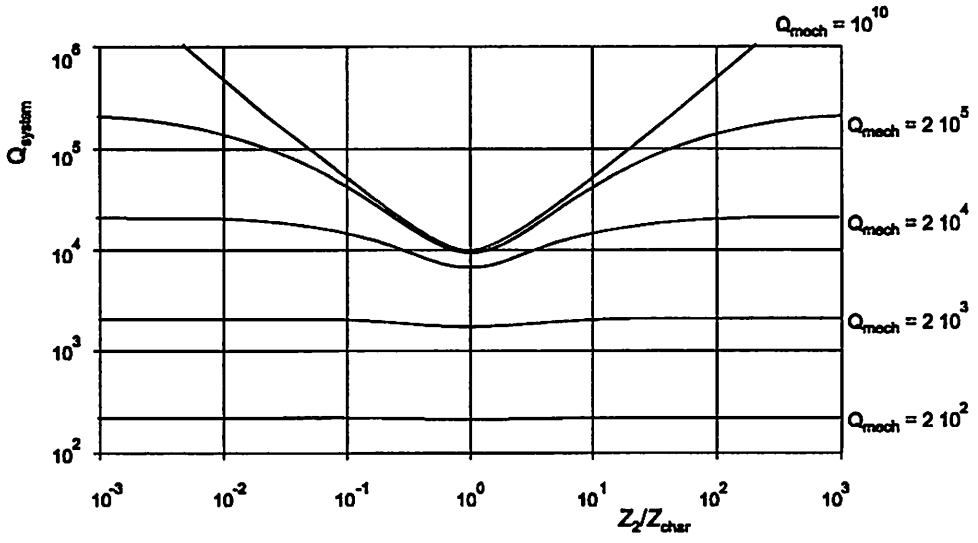

Fig. 6.3.2: Q-factor of the piezoelectrically operated force sensor as a function of the load impedance at the electrical ports for various values of the mechanical Q.

6.3.3 Electrostatically operated resonators

The coupling factor of a resonator with an electrostatic mechanism using an air-gap can be considerably higher as the coupling factor of the piezoelectric device discussed in the previous subsection. The coupling factor can be controlled from 0 to 1 by increasing the bias voltage from 0 to the pull-in value (see chapter 5.II). Hence, the Q due electrical dissipation will be considerably lower for load impedances around the characteristic impedance. In fig. 6.3.3, the loaded Q is shown for an electrostatic resonator as a function of the bias voltage. This is done for several values of Z_2/Z_{char}. It is assumed that the mechanical Q is infinite. The figure shows that, even for a relative large impedance mismatch (e.g. a factor 100), Q's are lower than 10^4 at moderate bias voltages (e.g. 25% of the pull-in voltage). Mechanical Q's of vacuum encapsulated electrostatically operated resonators can be in this regime, thus for such devices, it is not unimaginable that the system Q is determined by electrical dissipation.

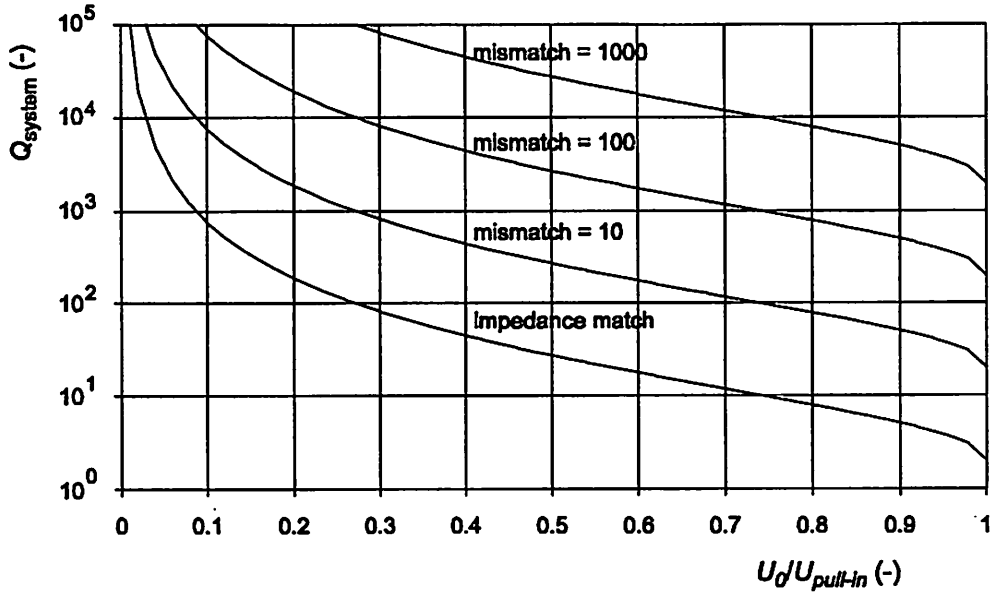

Fig. 6.3.3: System Q of an electrostatically operated resonator as a function of the normalized bias voltage for various values of the impedance mismatch Z_2/Z_{char}. The mechanical Q is assumed infinite: the system Q is completely determined by electrical dissipation.

References to 6.3

[1] F.R. Blom, *Resonant silicon beam force sensor*, PhD Thesis, University of Twente, the Netherlands (1989).

[2] C.J. van Mullem, *Micromachined silicon integrated resonant sensors*, PhD Thesis, University of Twente, the Netherlands (1993).

6.4 Shifts of the resonance frequency by fluid-mass loading

In section 6.2, the effect of a changing gas (fluid) environment on the quality factor has been described. It is a well known phenomenon that the resonance frequency of a second order vibrating system changes as a function of the quality factor. The relative change of the resonance frequency equals $\Delta f/f_{res} = 1/(1-1/4Q^2)^{1/2}$. For Q's of several hundreds or thousands this change becomes very small and can be neglected.

However, there is yet another unwanted effect of a changing gas environment which causes a much larger change of the resonance frequency: In fact, the effective mass of the vibrating structure is larger than the mass of the structure itself because the surrounding medium, which is set in vibration by the resonator, also contributes to the effective mass. This additive mass causes a shift of the resonance frequency. This shift is variable if the density of the surrounding medium is subject to changes. This effect is one of the main disadvantages of resonating membrane differential pressure sensors: the frequency of the membrane is not only determined by the differential pressure, but also by the density of the surrounding gas. To avoid this effect, resonators should be placed in (vacuum) encapsulated cavities with, such that they vibrate in a well defined, non-changing environment.

This mass loading phenomenon of vibrating diaphragms has been dealt with in [1], and references therein

reference

[1] A. Prak, F.R. Blom, M. Elwenspoek and T.S.J. Lammerink, *Q-factor and frequency shift of resonating silicon diaphragms in air,* Sensors and Actuators A, 25-27 (1991) 691-698.

6.5 Non-linear (large amplitude) effects [3]

In the derivation of the equation of motion (3.1), small amplitudes of the vibration w_{max} were assumed. If w_{max} becomes comparable to the radius of gyration $r=\sqrt{(I/A)}$ of the cross section of the beam, the dependence of the axial force on the amplitude of the vibration has to be taken into account resulting in a non-linear term [. 56]. If the distance between the ends of the beam is rigidly fixed, a tensile axial force will be developed by the transverse deflection. This will result in an increase of the resonant frequencies of the beam and is known in the literature as the "hard-spring effect" [. 56- .61]. To get some idea of the impact of this effect on the natural frequencies, an additional potential energy term is included in Rayleigh's quotient. The additional stretching of the midplane of the beam results in a potential energy change U_{NL} given by

$$U_{NL} = \frac{1}{2}\int_0^l \frac{EA}{4}\left(\frac{dw}{dx}\right)^4 dx \qquad (.20)$$

Including this term in Rayleigh's quotient results in a modified expression of eq. (3.24):

$$\omega_n(N,w_{max}) = \omega_n(0,0)\sqrt{1+\gamma_n\frac{Nl^2}{12\hat{E}I}+\beta_n\frac{EA}{12\hat{E}I}w_{max}^2} \qquad (.21)$$

where $\omega_n(0,0)$ is the natural frequency of mode n for zero-axial load and ignoring non-linear effects, w_{max} the amplitude of the vibration and β_n a constant given by

$$\beta_n = \frac{3}{\tilde{\phi}_{n,max}^2}\left[\int_0^l\left(\frac{d\tilde{\phi}_n(x)}{dx}\right)^4 dx \Big/ \int_0^l\left(\frac{d^2\tilde{\phi}_n(x)}{dx^2}\right)^2 dx\right] \qquad (22)$$

---

[3] From: H.A.C. Tilmans, *Micromechanical sensors using encapsulated built-in resonant strain gauges*, PhD Thesis chapter 2.4, Univ. of Twente, Enschede, the Netherlands (1993)
Also published in: H.A.C. Tilmans, M. Elwenspoek and J.H.J. Fluitman, *Micro resonant force gauges*, Sensors and Actuators A 30 (1992), 35-53.

where $\tilde{\phi}_{n,max}$ is the maximum value of the approximate shape function $\tilde{\phi}_n$. For prismatic, wide beams with a rectangular cross section and $N=bhE\varepsilon$, eq. (21) can be written as

$$\omega_n(\varepsilon,w_{max}) = \frac{\alpha_n^2}{\sqrt{12}}\left(\frac{E}{\rho(1-\nu^2)}\right)^{\frac{1}{2}}\frac{h}{l^2}\left[1+\gamma_n\varepsilon(1-\nu^2)\left(\frac{l}{h}\right)^2+\beta_n(1-\nu^2)\left(\frac{w_{max}}{h}\right)^2\right]^{\frac{1}{2}} \qquad (23)$$

The dependence of the resonant frequency on the amplitude of vibration given by eq. (23) is similar in form to the frequency dependence of a simple spring-mass system with a restoring force having a cubic dependence on the vibration amplitude. An estimate for the coefficients β_1 and β_2 of the fundamental mode and first harmonic, respectively, can be found by substituting the mode shapes for zero-axial force into eq. (22). This yields: $\beta_1=0.528$ and $\beta_2=1.228$ for a prismatic clamped-clamped beam, with a rectangular cross section. The coefficient β_n depends on the edge conditions of the beam, e.g., for simply supported edges β_n will be higher. In the case of movable axial end supports, the *hardening* effect will be smaller and can even revert to a *softening* effect for beams with a sufficiently small aspect ratio l/h [.57]. The dependence of the resonant frequency on the vibrational amplitude of the fundamental mode of a rigidly clamped-clamped beam, together with a typical large amplitude *forced response plot* is shown in Fig. .4.

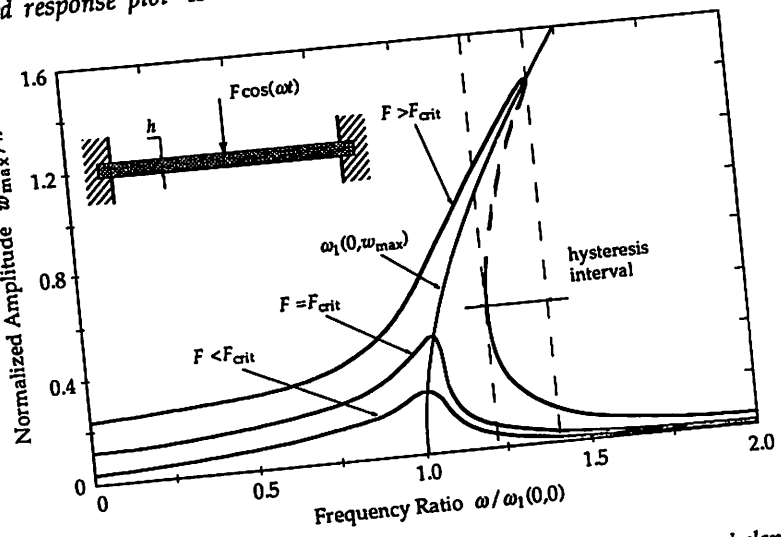

Fig. 4. Normalized amplitude versus the normalized frequency for a clamped-clamped beam with a rectangular cross section and with zero built-in axial strain. If the magnitude F of the excitation force exceeds a critical value F_{crit}, the amplitude becomes 3-valued in a particular frequency interval. The dashed part of the curve in this interval indicates unstable points [2.61].

Figure 4 also indicates the effect of the magnitude of the driving force on t[illegible] response plot [. 61]. If the magnitude of the driving force exceeds a critical value F_{crit} the amplitude becomes 3-valued within a range of frequencies. This frequency interval defines the region of hysteresis, with two stable points, one [illegible]int at a large amplitude and the other at a small amplitude. To avoid [illegible]/steresis, the magnitude of the driving force should be smaller than the critical load. It can be shown that the critical load is inversely proportional to [illegible]3/2, where Q the quality factor of the resonator [.61]. At the critical load, the [illegible]mplitude of vibration is defined as the critical amplitude $w_{max.crit}$, being inversely proportional to $Q^{1/2}$. Considering a clamped-clamped beam to [illegible]ehave as a simple spring-mass system with a restoring force having a cubic [illegible]ependence on the amplitude, it can be shown [.61] that the critical amplitude can be approximated by: $w_{max.crit}/h \approx \sqrt{[2/(Q\beta_n(1-\nu^2)]}$. Hence, even though a [illegible]high Q has several advantages as indicated in the previous section, it enhances the chance for hysteresis to occur.

Noise or other instabilities of the vibrational amplitude will limit the ulti[illegible]mate frequency resolution or stability of the gauge. Any frequency change caused by an amplitude change must be small compared to the minimum frequency change one wishes to resolve. It can be derived from eqns. and (. 23), that a condition, which defines an upper limit for the variations Δw_{max} in the amplitude is given by

$$\left(\frac{\Delta w_{max}}{w_{max}}\right) \ll \left(\frac{\gamma_n}{2\beta_n G_{\varepsilon n}}\right)\left(\frac{l}{h}\right)^2\left(\frac{h}{w_{max}}\right)^2\left(\frac{\Delta\omega}{\omega}\right)_{min} \qquad (w_{max} < w_{max,crit}) \qquad (24)$$

where $(\Delta\omega/\omega)_{min}$ is the minimum resolution required. For a clamped-clamped beam with an aspect ratio $l/h=200$, $h/w_{max}=500$, zero residual strain ($\varepsilon_0=0$) and a minimum frequency resolution of 10^{-6} eq. (.24) demands a relative variation of the maximum amplitude much smaller than 0.5. If the beam thickness $h=1\,\mu m$, this means that $w_{max}=2\,nm$ and $\Delta w_{max} \ll 0.5\,nm$. The critical amplitude in this case is approximately equal to 20 nm for $Q=10^4$.

.56 J. G. Eisley, Nonlinear vibration of beams and rectangular plates, *J. of Appl. Mathematics and Physics*, 15 (1964) 167-175.

.57 C. Mei and K. Decha-Umphai, A finite element method for non-linear forced vibrations of beams, *J. Sound and Vibration*, 102 (1985) 369-380.

58 M. V. Andres, K. W. H. Foulds and M. J. Tudor, Nonlinear vibrations and hysteresis of micromachined silicon resonators designed as frequency-out sensors, *Electron. Lett.* 23 (1987) 952-954.

59 K. Ikeda, H. Kuwayama, T. Kobayashi, T. Watanabe, T. Nishikawa, T. Yoshida and K. Harada, Study of nonlinear vibration of silicon resonant beam strain gauge, *Proc. of the 8th Sensor Symp., Tokyo, Japan, 1989*, pp. 21-24.

60 J. D. Zook, D. W. Burns, H. Guckel, J. J. Sniegowski, R. L. Engelstad and Z. Feng, Resonant microbeam strain transducers, *Proc. 6th Int. Conf. Solid-State Sensors and Actuators (Transducers '91), San Francisco, U.S.A., June 24-27, 1991*, pp. 529-532.

61 L. D. Landau and E. M. Lifschitz, *Lehrbuch der theoretischen physik-Mechanik*, Akademie-Verlag-Berlin, 3rd edn., 1964, pp. 101-104.

6.6 Modulating bias effects and 2ω components

Some excitation and detection mechanisms need a bias signal in order to work. For the electrostatic mechanisms, this is very clear, since the electromechanical coupling terms in the constituent equations (see section 5.I) are proportional to the squared bias voltage. This bias voltage causes a static deflection of the beam, which results in an elongation and bending of the neutral plane, and thus in an axial stress. This stress causes a shift of the resonance frequency, and thus a change of the modal spring constants K_j. The bias voltage modifies the system parameters, and thus the matrix elements of the constituent equation: the system becomes inherently nonlinear. In order to solve the problem, an additional term representing the strain energy has to be included in the energy function. This term equals:

$$E_{strain} = \frac{1}{8} E_b w_b h_b \int_0^l \sum_j (y_j v_j')^4 dx \tag{1}$$

Evaluation of this expression yields the following correction to be made on the spring constant K_1:

$$K_1' = K_1 \left(1 + \left(\frac{2.86}{f} \frac{y_{1,0}}{h_b} \right)^2 \right) \tag{2}$$

where $y_{1,0}$ is the static deflection due to the bias voltage, and f the ratio of the resonance frequency with and without an *initial* strain, that is the strain which is present in the *uncurved* beam ($y_{1,0}$=0). The increase in resonance frequency due to stretching of the neutral plane is proportional to the bias voltage u_0.

Another problem of this kind is the thermal heating that goes with many mechanisms. In order to obtain a harmonic component, the dynamic heating power of the thermal excitation mechanisms always has to be superimposed on a static heating power. Static heating also occurs in the piezoresistive detection mechanism, the optical detection techniques, and the magnetic mechanism although in the last one no bias current is necessary. The consequences of the static heating depend very much on the thermal properties of the applied materials and the geometry of the resonator and its surroundings. A direct consequence is that temperature dependent quantities like Young's modulus will change (this will be discussed in 6.7). In layered structures, bending moments can occur due to differences in thermal expansion coefficients of the materials. Another phenomenon shows up when the temperature of the resonator rises more than that of its surroundings. In that case, a compressive strain occurs in the resonator, which has consequences for the resonance frequency. This phenomenon is described in [1] and [2]. In most sensor designs this phenomenon is experienced as inconvenient, however the thermally excited mass-flow sensor described in [3], [4] works due to this principle.

The reason why bias signals are required is often that the physical effects on which the mechanisms are based are quadratic effects. This means that besides the static component (some consequences of which are discussed above) and the desired component with frequency ω, there also is a 2ω component:

$$(u_0 + \bar{u}e^{j\omega t})^2 = (u_0^2 + \tfrac{1}{2}\bar{u}^2) + 2u_0\bar{u}e^{j\omega t} + \tfrac{1}{2}\bar{u}^2 e^{j2\omega t} \qquad (3)$$

In practice, the 2ω components can be kept small by using relative high bias signals. Besides, they generally do not match higher harmonics since the ratio of the resonance frequencies are generally not integers, as for example in the case of a stretched wire. An elegant way to suppress 2ω components is to use an anharmonic drive signal which, when squared, results in a static and ω component only.

references to 6.6

[1] T.S.J. Lammerink, M. Elwenspoek, R.H. van Ouwerkerk, S. Bouwstra and J.H.J. Fluitman, *Performance of thermally excited resonators*, Sensors and Actuators, A21-A23 (1990), 352-356.

[2] L.M. Zhang, D. Walsh, D. Uttamchandani and B. Culshaw, *Effect of optical power on the resonance frequency of optically powered silicon microresonators*, Sensors and Actuators A, 29 (1991), 73-78.

[3] H.J.M. Geijselaers and H. Tijdeman, *The dynamic mechanical characteristics of a resonating microbridge mass-flow sensor*, Sensors and Actuators A, 29 (1991), 37-41.

[4] S. Bouwstra, R. Legtenberg, H.A.C. Tilmans and M. Elwenspoek, *Resonating microbridge mass flow sensor*, Sensors and Actuators, A21-A23 (1990), 332-335.

6.7 Temperature dependence of the resonance frequency

The temperature dependence of the resonance frequency of pure silicon beams in the temperature range -55 to +105 °C (218 to 378 K) is given. This range corresponds to the military temperature range.

For the resonance frequency of a pure silicon beam, without an axial load, one can write:

$$f_r = c \sqrt{\frac{\varrho}{\hat{E}}} \frac{t}{l^2} \qquad (1)$$

where
ϱ is the density of silicon
t is the thickness of the beam
l is the length of the beam
$\hat{E}$ is the effective youngs modulus for bending of the beam
$\hat{E} = E$ for beams with thickness and width of the same order
$\hat{E} = E(1-\nu^2)$ for flat beams (thickness << width)
ν is the poissons ratio
c is a constant, depending on the boundary conditions

All parameters, except c show a temperature dependence:

$$t = t_0 \left(1 + \int_{T0}^{T} \alpha(T)dT\right); \qquad l = l_0 \left(1 + \int_{T0}^{T} \alpha(T)dT\right); \qquad \varrho = \varrho_0 \left(1 - 3\int_{T0}^{T} \alpha(T)dT\right)$$

$$\hat{E} = \hat{E}_0 \left(1 + \int_{T0}^{T} \frac{1}{\hat{E}(T)} \frac{\partial \hat{E}(T)}{\partial T} dT\right) \qquad (2)$$

where $\alpha(T)$ is the temperature dependent expansion coefficient of silicon. Subscript 0 refers to a reference temperature, e.g. 20 °C. By substituting eqns (2) into (1), and assuming small values for the relative changes of the parameters we obtain

$$f_r = f_{r,0} \left(1 + \frac{1}{2}\int_{T0}^{T} \alpha(T)dT + \frac{1}{2}\int_{T0}^{T} \frac{1}{\hat{E}(T)} \frac{\partial \hat{E}(T)}{\partial T} dT\right)$$

or:

$$\frac{\Delta f_r}{f_{r,0}} = \frac{1}{2}\int_{T0}^{T} \alpha(T)dT + \frac{1}{2}\int_{T0}^{T} \frac{1}{\hat{E}(T)} \frac{\partial \hat{E}(T)}{\partial T} dT) \qquad (3)$$

with $\Delta f_r = f_r - f_{r,0}$.

Values for the first integral in the temperature range 218 to 340 K can be found in [1]. From 340 to 378 K the integral can be calculated from [2]. To get a value for the second integral, the temperature dependence of the effective youngs modulus has to be known. For the Youngs modulus

along crystal axes, one can write [5]:

$$E = (C_{11}-C_{12})(C_{11}+2C_{12})/(C_{11}+C_{12})$$

The temperature dependencies of C_{11} and C_{12} are given in [6] and [4]. They are constant over the entire temperature range. Their values are:

$$\frac{1}{C_{11}}\frac{d\,C_{11}}{dT} = -94 \text{ ppm/K}$$

$$\frac{1}{C_{12}}\frac{d\,C_{12}}{dT} = -98 \text{ ppm/K}$$

The temperature dependencies of C_{11} and C_{12} are equal in good approximation, and therefore the temperature dependence of E will have the same value. For Poissons ratio we can write [5]:

$$\nu = C_{12}/(C_{11}+C_{12})$$

so in good approximation, Poissons ratio shows no temperature dependence. This means that the temperature dependence of slender and flat beams show the same temperature dependence.
The values of the integrals of (3) are listed below for various temperatures. 20 °C was choosen as a reference temperature

Table I

Temperature	$\frac{1}{2}\int_{T0}^{T}\alpha(T)dT$	$\frac{1}{2}\int_{T0}^{T}\frac{1}{\hat{E}(T)}\frac{\partial\hat{E}(T)}{\partial T}dT)$
(°C)	(ppm)	(ppm)
-60		3760
-50	-76	3290
-40	-67	2820
-30	-57	2350
-20	-48	1880
-10	-36	1410
0	-25	940
10	-12	470
20	0	0
30	13	-470
40	26	-940
50	40	-1410
60	54	-1880
70		-2350
80		-2850
90		-3290
100		-3760
110		-4230

From this table, we can conclude that contribution of the temperature dependence of youngs modulus is much larger than the temperature dependence of the density. The resonance frequency shifts almost linearly with the temperature with approximately 47 ppm/°C. When we compare this with the temperature dependence of AT-cut quarz crystal resonators, which have a temperature dependence of the resonance frequency of approx. 25 ppm over the entire temperature range [7], we have to conclude that the frequency stability of silicon resonators due to temperature variations is very poor.

6.7.1 Solutions

Temperature dependence of resonators is typically some 10 to 100 ppm/C if no measures are taken. There are a number of solutions to reduce the temperature dependence of the resonance frequency.

Temperature compensation

The sensor system consists of two resonators, one of which is sensitive to temperature as well as to the measurand, while the other is sensitive to the temperature only. By substracting the resonance frequency, temperature effects (and possibly also other unwanted phenomena) are eliminated [8]. Other designs use a configuration in which the two resonators have an opposite dependence on the measurand, while the temperature dependence of the two resonators is the same [9]. A very elegant way of temperature compensation is shown in [10]. When a certain amount of gas is enclosed in the hollow resonator, the stiffnes reduction by Young's modulus is compensated by stiffness increase caused by the pressure. The resulting temperature dependence is 1.3 ppm/C.

Temperature control

An other way to eliminate temperature effects is to keep the resonator at constant temperature: the signal from a temperature sensor is fed back to a heating resistor in the vicinity of the resonator [11]. Of course, one needs not to realize the tempoerature controll unit in a micromechanical way: it is much simpler to place the resonator in a oven.

Temperature correction

May be the simplest way temperature effects can be eliminated is when you *know* the effect of the temperature on the resonance frequency, for instance by running a calibration procedure before the sensor is sold. Temperature-measurand-frequency data can be stored in a lookup table. By measuring the temperature (e.g. using a pn-junction) and resonance frequency, the value of the measurand can be obtained from that table. The two commercial silicon resonant sensors (i.e. the Druck-sensor and the Yokogawa sensor, see chapter 8) both use this way to reduce temperature efects.

References to 6.7

[1] K.G. Lyon et. al., Linear thermal expansion measurements on silicon from 6 to 340 K, J. Appl. Phys., 48(3), 865-8, 1977

[2] Y. Okada et. al., Precise determination of lattice parameter and thermal expansion coefficient of silicon between 300 and 1500 K.

[3] J.J. Hall, Electronic effects in the elastic constants of *n*-type silicon, Phys. Rev., 161(3), 756 - 761, 1967

[4] Landolt - Bornstein Crystal and solid state physics ed. K.-H. Hellwege vol. 11 (springer 1979) p. 116

[5] A. Heuberger, Mikromechanik, Springer Verlag (1989) p. 41

[6] Properties of silicon, INSPEC (1988), p. 15

[7] M.E. Frerking, Crystal oscillator design and temperature compensation, Van Nostrand Reinhold Company (1978), p. 27.

[8] K. Seibert, D. Largeau, B. Bonvalot, D.T. Angelidis and P. Parsons, *Optical system for pressure and temperature sensing,* Proc. IEEE Conf. Solid State Sensors and Actuators 1993 (Transducers 93), 7-10 June 1993, Yokohama, Japan, 690.

[9] H.A.C. Tilmans, S. Bouwstra, D.J. Yntema, M. Elwenspoek and C.F. Klein, *A differential resonator design using a bossed structure for applications in mechanical sensors*, Sensors and Actuators A, 25-27 (1991), 385-393.

[10] E. Stemme and G. Stemme, *A capacitively excited and detected resonant pressure sensor with temperature compensation*, Sensors and Actuators A, 31 (1992), 639-647.

[11] C.T.-C. Nguyen and R.T. Howe, *Microresonator frequency control and stabilization using an integrated microoven,* Proc. IEEE Conf. Solid State Sensors and Actuators 1993 (Transducers 93), 7-10 June 1993, Yokohama, Japan, 1040.